



# International Journal of Engineering Researches and Management Studies

## SPECTRAL AND THERMAL PROPERTIES OF HO<sup>3+</sup> DOPED OXY-FLUORIDE GLASSES

S. L. Meena

Ceremic Laboratory, Department of physics, Jai Narain Vyas University, Jodhpur 342001(Raj.) India

### ABSTRACT

Lead cadmium antimony silicate oxy-fluoride glasses containing Ho<sup>3+</sup> in (40- x): SiO<sub>2</sub>: 10PbF<sub>2</sub>: 10PbO: 10CdF<sub>2</sub>:30Sb<sub>2</sub>O<sub>3</sub>:xHo<sub>2</sub>O<sub>3</sub> (where x=1, 1.5,2 mol %) have been prepared by melt-quenching method. The amorphous nature of the glasses was confirmed by x-ray diffraction studies. Optical absorption spectra were recorded at room temperature for all glass samples. The experimental oscillator strengths were calculated from the area under the absorption bands. Slater-Condon parameter F<sub>2</sub>, Lande's parameter  $\xi_{4f}$ , Nephelauxetic ratio ( $\beta'$ ) and Bonding parameter ( $b^{1/2}$ ) have been computed. Using these parameters energies and intensities of these bands has been calculated. Judd-Ofelt intensity parameters  $\Omega_{\lambda}$  ( $\lambda=2, 4, 6$ ) are evaluated from the intensities of various absorption bands of optical absorption spectra. Using these intensity parameters various radiative properties like spontaneous emission probability, branching ratio, radiative life time and stimulated emission cross-section of various emission lines have been evaluated

**KEYWORDS:** Oxy-fluoride Glasses, Optical Properties, Judd-Ofelt Theory, Rare earth ions.

### 1. INTRODUCTION

Rare earth doped materials have gained great interest in the decade for their use solid state lasers, optoelectronic devices and solar cells [1-4]. Oxy-fluoride glasses have smaller multiphonon emission rates and are chemically stable. They are also stable against atmospheric moisture [5-8]. Lead cadmium antimony silicate oxyfluoride glasses find a wide range of technological applications as electro-chemical devices as ionic conductors [9, 10]. Oxy-fluoride glasses have been considered as promising host materials due to their high transparency and low phonon energy[11-13]. Among RE<sup>3+</sup> ions, Ho<sup>3+</sup> is an interesting ion for spectroscopic studies, because it exhibits several electronic transitions in the UV and VIS.

In this work, we have studied on the absorption and emission properties of Ho<sup>3+</sup> doped Lead cadmium antimony silicate oxy-fluoride glasses. The Judd-Ofelt theory has been applied to compute the intensity parameters  $\Omega_{\lambda}$  ( $\lambda=2, 4, 6$ ), which are sensitive to the environment of rare earth ion. From these parameters, important optical properties such as radiative transition probability for spontaneous emission, radiative lifetime of the excited states and branching ratio can be estimated.

### 2. EXPERIMENTAL TECHNIQUES

#### Preparation of glasses

The following Ho<sup>3+</sup> doped lead cadmium antimony silicate oxy fluoride glass samples (40- x): SiO<sub>2</sub>: 10PbF<sub>2</sub>: 10PbO: 10CdF<sub>2</sub>:30Sb<sub>2</sub>O<sub>3</sub>:xHo<sub>2</sub>O<sub>3</sub> (where x=1, 1.5,2) have been prepared by melt-quenching method. Analytical reagent grade chemical used in the present study consist of SiO<sub>2</sub>, PbF<sub>2</sub>, PbO, CdF<sub>2</sub>, Sb<sub>2</sub>O<sub>3</sub> and Ho<sub>2</sub>O<sub>3</sub>. All weighed chemicals were powdered by using an Agate pestle mortar and mixed thoroughly before each batch (10g) was melted in alumina crucibles in silicon carbide based an electrical furnace.

Silicon Carbide Muffle furnace was heated to working temperature of 1050<sup>0</sup>C, for preparation of Lead cadmium antimony silicate oxy-fluoride glasses, for two hours to ensure the melt to be free from gases. The melt was stirred several times to ensure homogeneity. For quenching, the melt was quickly poured on the steel plate & was immediately inserted in the muffle furnace for annealing. The steel plate was preheated to 100<sup>0</sup>C. While pouring; the temperature of crucible was also maintained to prevent crystallization. And annealed at temperature of 250<sup>0</sup>C for 2h to remove thermal strains and stresses. Every time fine powder of cerium oxide was used for polishing the samples. The glass samples so prepared were of good optical quality and were transparent. The chemical compositions of the glasses with the name of samples are summarized in **Table 1**



# International Journal of Engineering Researches and Management Studies

*Table 1 Chemical composition of the glasses*

Sample	Glass composition (mol %)
LCASO (UD)	40 SiO <sub>2</sub> : 10PbF <sub>2</sub> : 10PbO: 10CdF <sub>2</sub> : 30Sb <sub>2</sub> O <sub>3</sub>
LCASO (HO1)	39 SiO <sub>2</sub> : 10PbF <sub>2</sub> : 10PbO: 10CdF <sub>2</sub> : 30Sb <sub>2</sub> O <sub>3</sub> : 1 Ho <sub>2</sub> O <sub>3</sub>
LCASO (HO1.5)	38.5 SiO <sub>2</sub> : 10PbF <sub>2</sub> : 10PbO: 10CdF <sub>2</sub> : 30Sb <sub>2</sub> O <sub>3</sub> : 1.5 Ho <sub>2</sub> O <sub>3</sub>
LCASO (HO2)	38 SiO <sub>2</sub> : 10PbF <sub>2</sub> : 10PbO: 10CdF <sub>2</sub> : 30Sb <sub>2</sub> O <sub>3</sub> : 2 Ho <sub>2</sub> O <sub>3</sub>

LCASO (UD)-Represents undoped Lead cadmium antimony silicate oxy-fluoride specimens

LCASO (HO) -Represents Ho<sup>3+</sup> doped Lead cadmium antimony silicate oxy-fluoride specimens

### 3. THEORY

#### 3.1 Oscillator Strength

The intensity of spectral lines is expressed in terms of oscillator strengths using the relation [14].

$$f_{\text{expt.}} = 4.318 \times 10^{-9} \int \epsilon(\nu) d\nu \quad (1)$$

where,  $\epsilon(\nu)$  is molar absorption coefficient at a given energy  $\nu$  (cm<sup>-1</sup>), to be evaluated from Beer–Lambert law.

Under Gaussian Approximation, using Beer–Lambert law, the observed oscillator strengths of the absorption bands have been experimentally calculated, using the modified relation [15].

$$P_m = 4.6 \times 10^{-9} \times \frac{1}{cl} \log \frac{I_0}{I} \times \Delta\nu_{1/2} \quad (2)$$

where  $c$  is the molar concentration of the absorbing ion per unit volume,  $l$  is the optical path length,  $\log I_0/I$  is optical density and  $\Delta\nu_{1/2}$  is half band width.

#### 3.2. Judd-Ofelt Intensity Parameters

According to Judd [16] and Ofelt [17] theory, independently derived expression for the oscillator strength of the induced forced electric dipole transitions between an initial  $J$  manifold  $|4f^N(S, L) J\rangle$  level and the terminal  $J'$  manifold  $|4f^N(S', L') J'\rangle$  is given by:

$$\frac{8\pi^2 mc \bar{\nu}}{3h(2J+1)n} \left[ \frac{(n^2+2)^2}{9} \right] \times S(J, J') \quad (3)$$

where, the line strength  $S(J, J')$  is given by the equation

$$S(J, J') = e^2 \sum_{\lambda=2, 4, 6} \Omega_{\lambda} \langle 4f^N(S, L) J \| U^{(\lambda)} \| 4f^N(S', L') J' \rangle^2 \quad (4)$$

In the above equation  $m$  is the mass of an electron,  $c$  is the velocity of light,  $\nu$  is the wave number of the transition,  $h$  is Planck's constant,  $n$  is the refractive index,  $J$  and  $J'$  are the total angular momentum of the initial and final level respectively,  $\Omega_{\lambda}$  ( $\lambda = 2, 4, 6$ ) are known as Judd-Ofelt intensity parameters.

#### 3.3. Radiative Properties

The  $\Omega_{\lambda}$  parameters obtained using the absorption spectral results have been used to predict radiative properties such as spontaneous emission probability ( $A$ ) and radiative life time ( $\tau_R$ ), and laser parameters like fluorescence branching ratio ( $\beta_R$ ) and stimulated emission cross section ( $\sigma_p$ ).

The spontaneous emission probability from initial manifold  $|4f^N(S', L') J'\rangle$  to a final manifold  $|4f^N(S, L) J\rangle$  is given by:

$$A[(S', L') J'; (S, L) J] = \frac{64 \pi^2 \nu^3}{3h(2J'+1)} \left[ \frac{n(n^2+2)^2}{9} \right] \times S(J', \bar{J}) \quad (5)$$



# International Journal of Engineering Researches and Management Studies

Where,  $S(J, J) = e^2 [\Omega_2 \|U^{(2)}\|^2 + \Omega_4 \|U^{(4)}\|^2 + \Omega_6 \|U^{(6)}\|^2]$

The fluorescence branching ratio for the transitions originating from a specific initial manifold  $|4f^N(S', L') J' \rangle$  to a final manifold  $|4f^N(S, L) J \rangle$  is given by

$$\beta_{[(S', L') J'; (S, L) J]} = \frac{A[(S', L) J; (\bar{S}, \bar{L}) \bar{J}]}{\sum_{S L J} A[(S', L) J; (\bar{S}, \bar{L}) \bar{J}]} \quad (6)$$

where, the sum is over all terminal manifolds.

The radiative life time is given by

$$\tau_{rad} = \sum_{S L J} A[(S', L) J'; (S, L) J] = A_{Total}^{-1} \quad (7)$$

where, the sum is over all possible terminal manifolds. The stimulated emission cross-section for a transition from an initial manifold  $|4f^N(S', L') J' \rangle$  to a final manifold  $|4f^N(S, L) J \rangle$  is expressed as

$$\sigma_p(\lambda_p) = \left[ \frac{\lambda_p^4}{8\pi c n^2 \Delta\lambda_{eff}} \right] \times A[(S', L') J'; (\bar{S}, \bar{L}) \bar{J}] \quad (8)$$

where,  $\lambda_p$  the peak fluorescence wavelength of the emission band and  $\Delta\lambda_{eff}$  is the effective fluorescence line width.

### 3.4 Nephelauxetic Ratio ( $\beta'$ ) and Bonding Parameter ( $b^{1/2}$ )

The nature of the R-O bond is known by the Nephelauxetic Ratio ( $\beta'$ ) and Bonding Parameter ( $b^{1/2}$ ), which are computed by using following formulae [18, 19]. The Nephelauxetic Ratio is given by

$$\beta' = \frac{\nu_g}{\nu_a} \quad (9)$$

where,  $\nu_a$  and  $\nu_g$  refer to the energies of the corresponding transition in the glass and free ion, respectively. The values of bonding parameter ( $b^{1/2}$ ) are given by

$$b^{1/2} = \left[ \frac{1-\beta'}{2} \right]^{1/2} \quad (10)$$

## 4. RESULT AND DISCUSSION

### 4.1 XRD Measurement

Figure 1 presents the XRD pattern of the samples containing show no sharp Bragg's peak, but only a broad diffuse hump around low angle region. This is the clear indication of amorphous nature within the resolution limit of XRD instrument.

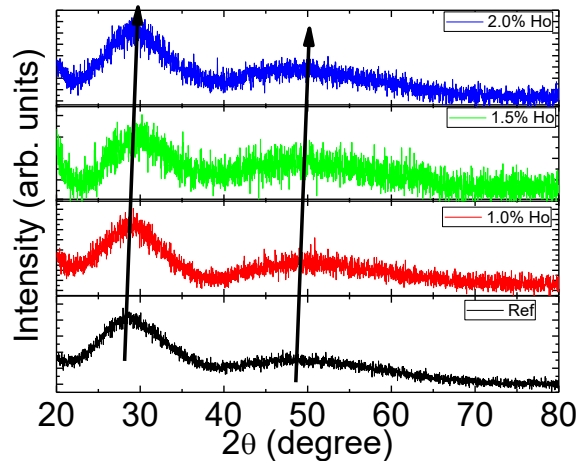
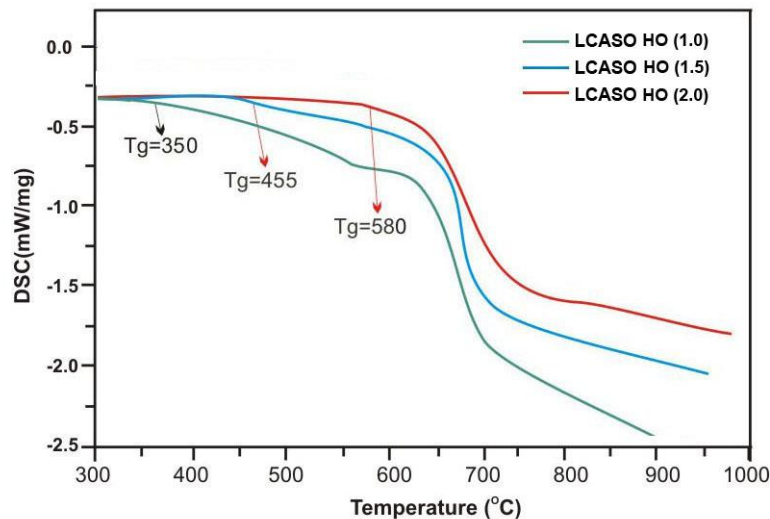


Fig.1: X-ray diffraction pattern of LCASO (HO) glasses

#### 4.2 Thermal Properties

Figure 2 shows the thermal properties of LCASO glass from 300<sup>o</sup>C to 1000<sup>o</sup>C. From the DSC curve of present glasses system, we can find out that no crystallization peak is apparent and the glass transition temperature  $T_g$  are 350<sup>o</sup>C, 455<sup>o</sup>C and 580<sup>o</sup>C respectively. The  $T_g$  increase with the contents of  $Ho_2O_3$  increase. We could conclude that thermal properties of the LCASO glass are good for fiber drawing from the analysis of DSC curve.



#### 4.3. Absorption spectra

The absorption spectra of LCASO (HO) glasses, consists of absorption bands corresponding to the absorptions from the ground state  $^5I_8$  of  $Ho^{3+}$  ions. Twelve absorption bands have been observed from the ground state  $^5I_8$  to excited states  $^5I_5$ ,  $^5I_4$ ,  $^5F_5$ ,  $^5F_4$ ,  $^5F_3$ ,  $^3K_8$ ,  $^5G_6$ ,  $(5G,3G)_5$ ,  $^5G_4$ ,  $^5G_2$ ,  $^5G_3$ , and  $^3F_4$  for  $Ho^{3+}$  doped LCASO (HO) glasses.



LCASO HO (01)

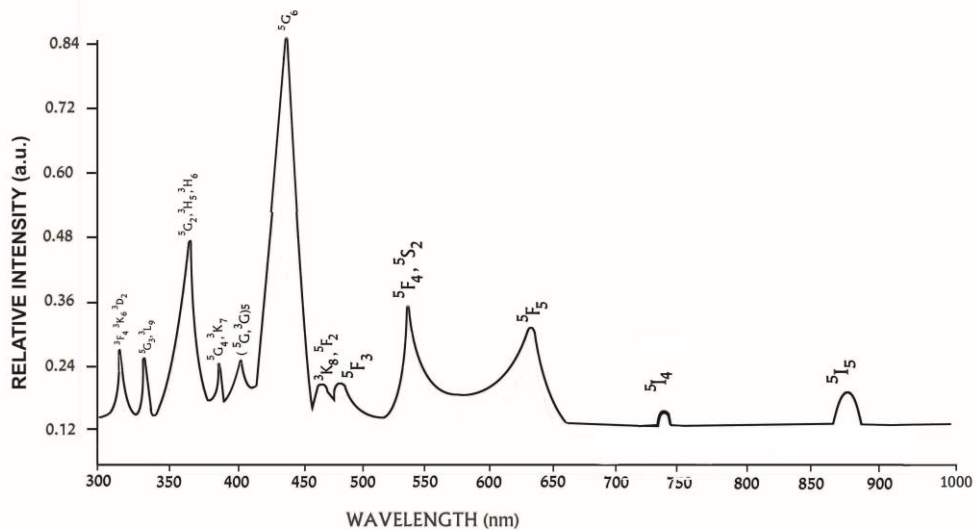


Fig.3: UV-VIS absorption spectra of LCASO (HO) glasses

The experimental and calculated oscillator strengths for Ho<sup>3+</sup> ions in Lead cadmium antimony silicate oxyfluoride glasses are given in **Table 2**

Table 2. Measured and calculated oscillator strength ( $P^m \times 10^{+6}$ ) of Ho<sup>3+</sup> ions in LCASO glasses.

Energy level	Glass LCASO (HO01)		Glass LCASO (HO1.5)		Glass LCASO (HO02)	
	P <sub>exp.</sub>	P <sub>cal.</sub>	P <sub>exp.</sub>	P <sub>cal.</sub>	P <sub>exp.</sub>	P <sub>cal.</sub>
<sup>5</sup> I <sub>5</sub>	0.48	0.24	0.45	0.24	0.42	0.23
<sup>5</sup> I <sub>4</sub>	0.07	0.02	0.05	0.02	0.04	0.02
<sup>5</sup> F <sub>5</sub>	3.48	2.74	3.42	2.71	3.39	2.69
<sup>5</sup> F <sub>5</sub> , <sup>5</sup> S <sub>2</sub>	4.62	4.27	4.58	4.22	4.55	4.20
<sup>5</sup> F <sub>3</sub>	1.56	2.38	1.52	2.36	1.48	2.35
<sup>3</sup> K <sub>8</sub> , <sup>5</sup> F <sub>2</sub>	1.36	1.96	1.32	1.93	1.29	1.91
<sup>5</sup> G <sub>6</sub>	25.75	25.73	24.86	24.87	23.95	23.98
( <sup>5</sup> G, <sup>3</sup> G) <sub>5</sub>	3.66	1.63	3.62	1.61	3.57	1.59
<sup>5</sup> G <sub>4</sub> , <sup>3</sup> K <sub>7</sub>	0.09	0.60	0.07	0.59	0.05	0.59



## International Journal of Engineering Researches and Management Studies

${}^5G_2, {}^3H_5$	5.46	5.45	5.42	5.29	5.38	5.13
${}^5G_3, {}^3L_9$	1.45	1.39	1.41	1.36	1.37	1.35
${}^3F_4, {}^3K_6$	1.32	4.04	1.28	3.99	1.25	3.95
R.m.s.deviation	1.0631		1.0581		1.0543	

Computed values of ( $F_2$ ), Lande's parameter ( $\xi_{4f}$ ), Nephelauxetic ratio ( $\beta'$ ) and bonding parameter ( $b^{1/2}$ ) for  $\text{Ho}^{3+}$  doped LCASO glass specimen are given in **Table 3**.

**Table 3.**  $F_2, \xi_{4f}, \beta'$  and  $b^{1/2}$  parameters for Holmium doped glass specimen

Glass Specimen	$F_2$	$\xi_{4f}$	$\beta'$	$b^{1/2}$
$\text{Ho}^{3+}$	427.89	2196.01	0.9718	0.1187

Judd-Ofelt intensity parameters  $\Omega_\lambda$  ( $\lambda = 2, 4, 6$ ) were calculated by using the fitting approximation of the experimental oscillator strengths to the calculated oscillator strengths with respect to their electric dipole contributions. In the present case the three  $\Omega_\lambda$  parameters follow the trend  $\Omega_4 < \Omega_6 < \Omega_2$ . The values of Judd-Ofelt intensity parameters are given in **Table 4**.

**Table 4.** Judd-Ofelt intensity parameters for  $\text{Ho}^{3+}$  doped LCASO glass specimens.

Glass Specimen	$\Omega_2(\text{pm}^2)$	$\Omega_4(\text{pm}^2)$	$\Omega_6(\text{pm}^2)$	$\Omega_4/\Omega_6$	Ref.
LCASO HO01	5.835	1.191	1.998	0.5961	P.W.
LCASO HO1.5	5.609	1.174	1.978	0.5935	P.W.
LCASO HO02	5.374	1.160	1.967	0.5897	P.W.
NBFS(DY)	10.05	1.37	2.16	0.6343	[20]
PSB (DY)	5.81	1.13	2.68	0.4216	[21]
LBWB(DY)	5.603	0.851	1.674	0.5084	[22]
ZLBB (HO)	4.801	0.945	1.673	0.5649	[23]
LLBP (TB)	3.339	1.179	2.462	0.4789	[24]

#### 4.4. Fluorescence Spectrum

The fluorescence spectrum of  $\text{Ho}^{3+}$  doped in Lead cadmium antimony silicate oxy-fluoride glass is shown in Figure 4. There are two broad bands ( ${}^5F_4, {}^5S_2 \rightarrow {}^5I_8$ ) and ( ${}^5F_5 \rightarrow {}^5I_8$ ) respectively for glass specimens.

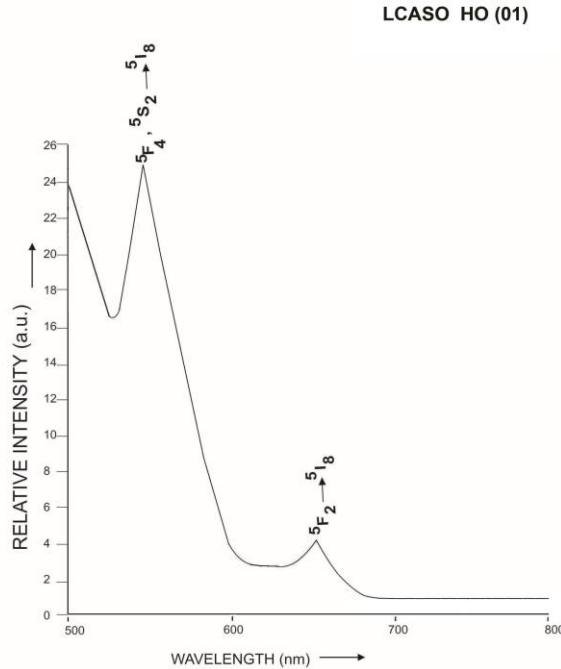


Fig.4: Fluorescence spectrum of LCASO glasses doped with Ho<sup>3+</sup>

Table 5. Emission peak wave lengths ( $\lambda_p$ ), radiative transition probability ( $A_{rad}$ ), branching ratio ( $\beta_R$ ), stimulated emission crosssection ( $\sigma_p$ ), and radiative life time ( $\tau_R$ ) for various transitions in Ho<sup>3+</sup> doped LCASO glasses.

Transition	LCASO (HO01)					LCASO (HO1.5)					LCASO (HO02)				
	$\lambda_p$ (nm)	$A_{rad}(s^{-1})$	$\beta_R$	$\sigma_p$ ( $10^{-20}cm^2$ )	$\tau_R$ ( $\mu s$ )	$A_{rad}(s^{-1})$	$\beta_R$	$\sigma_p$ ( $10^{-20}cm^2$ )	$\tau_R$ ( $\mu s$ )	$A_{rad}(s^{-1})$	$\beta_R$	$\sigma_p$ ( $10^{-20}cm^2$ )	$\tau_R$ ( $\mu s$ )		
$^5F_4, ^5S_2 \rightarrow ^5I_8$	555	5404.58	0.7220	1.118	133.6	5354.9	0.750	1.096	140.0	5328.0	0.750	1.084	140.7		
$^5F_5 \rightarrow ^5I_8$	652	2080.70	0.2780	1.074	0	1784.4	0.249	0.914	7	1774.8	0.249	0.897	9		
						0	9			3	8				

### 5. CONCLUSION

In the present study, the glass samples of composition (40- x): SiO<sub>2</sub>: 10PbF<sub>2</sub>: 10PbO: 10CdF<sub>2</sub>:30Sb<sub>2</sub>O<sub>3</sub>:xHo<sub>2</sub>O<sub>3</sub> (where x =1, 1.5, 2 mol %) have been prepared by melt-quenching method. The radiative transition probability, branching ratio are highest for ( $^5F_4, ^5S_2 \rightarrow ^5I_8$ ) transition and hence it is useful for laser action. The stimulated emission cross section ( $\sigma_p$ ) has highest value for the transition ( $^5F_4, ^5S_2 \rightarrow ^5I_8$ ) in all the glass specimens doped with Ho<sup>3+</sup> ion. This shows that ( $^5F_4, ^5S_2 \rightarrow ^5I_8$ ) transition is most probable transition.

### References

- [1] Charpentier, F., Stareek, F., Doualan, J L, Jovari, P., Camy, P., Troles, J.,Belin S., Bureau, B & Nazabal, V(2013). Mid-IR luminescence of Dy<sup>3+</sup> and Pr<sup>3+</sup> doped Ga5Ge20Sb10S (Se) 65 bulk glasses and fibers, Mater. Lett.101, 21.
- [2] Ying Guan, Zhihao Wei, Yanlin Huang, Ramzi Maalej & Hyo Jin Seo. (2013).1.55 $\mu m$  emission and up conversion luminescence of Er<sup>3+</sup>- doped strontium borate glasses. Ceramics International, 39, 7023.



## International Journal of Engineering Researches and Management Studies

- [3] Cai, J.E., Qiang, L., Ming, N.M., Hui, L., Xi, Y.H., Guo, G.Z. and Li, G.M. (2015). Spectroscopic properties of heavily  $\text{Ho}^{3+}$  doped barium yttrium fluoride crystals. *Chin. Phys. B*. Vol. 24, 094216-8
- [4] Weber, M. J. (1982). "Fluorescence and glass lasers," *J. Non-Cryst. Solids* 47, 117-134.
- [5] Weber, M. J. (1981). "Laser Excited Fluorescence Spectroscopy in Glass," in *Laser Spectroscopy of Solids*, W.M. Yen and P.M. Selzer, eds. (Springer, Berlin, pp. 189-239.
- [6] Adam, J. L. (2002). "Lanthanides in Non-Oxide Glasses," *Chem. Rev.* 102, 2461-2476.
- [7] Petrin, R. R., Kliwer, M. L., Beasley, J. Beasley, T., Powell, R. C., Aggarwal, I. D. and Ginther, R. C. (1991). "Spectroscopy and laser operation of Nd:ZBAN glass," *IEEE J. Quantum Electron.* QE-27, 1031-1038.
- [8] Azkargorta, J., Iparraguirre, I. Balda, R. Fernández, J., Dénoue, E. and Adam, J. (1994) "Spectroscopic and Laser Properties of  $\text{Nd}^{3+}$  in BiGaZLuTmN Fluoride Glass," *IEEE J. Quantum Electron.* 30, 1862-1867.
- [9] Mattarelli, M., Tikhomirov, V. K., Seddon, A. B., Montagna, M., Moser, E. Chiasera, A., Chausse, S., Nunzi Conti, G., Pelli, S., Righini, G.C., Zampedri, L. and Ferrari, M. (2004). "Tm<sup>3+</sup>-Activated Transparent Oxy-Fluoride Glass Ceramics: Structural and Spectroscopic Properties," *J. Non-Cryst. Solids*, 345-346, 354-58.
- [10] Fujihara, S., Kato, T. and Kimura, T. (2001). "Sol-Gel Synthesis of Silica-Based Oxyfluoride Glass-Ceramic Thin Films: Incorporation of  $\text{Eu}^{3+}$  Activators into Crystallites," *J. Am. Ceram. Soc.*, 84, 2716-18.
- [11] Yu, Y., Chen, D., Wang, Y., Liu, F. and Ma, E. Ma (2007). "A new transparent oxyfluoride glass ceramic with improved luminescence," *J. Non-Cryst. Solids*, 353, 405-09.
- [12] Bocker, C. and Rüssel, C. (2009) "Self-organized nano-crystallisation of BaF<sub>2</sub> from Na<sub>2</sub>O/K<sub>2</sub>O/BaF<sub>2</sub>/Al<sub>2</sub>O<sub>3</sub>/SiO<sub>2</sub> glasses," *J. Eur. Ceram. Soc.*, 29, 1221-25.
- [13] Margaryan, A., Choi, J. H., Shi, F. G. (2004) "Spectroscopic properties of  $\text{Mn}^{2+}$  in new bismuth and lead contained fluorophosphates glasses" *Appl. Phys. B* 78, p. 409.
- [14] Gorller-Walrand, C. and Binnemans, K. (1988) Spectral Intensities of f-f Transition. In: Gshneidner Jr., K.A. and Eyring, L., Eds., *Handbook on the Physics and Chemistry of Rare Earths*, Vol. 25, Chap. 167, North-Holland, Amsterdam, 101-264.
- [15] Sharma, Y.K., Surana, S.S.L. and Singh, R.K. (2009) Spectroscopic Investigations and Luminescence Spectra of  $\text{Sm}^{3+}$  Doped Soda Lime Silicate Glasses. *Journal of Rare Earths*, 27, 773-780.
- [16] Judd, B.R. (1962). Optical Absorption Intensities of Rare Earth Ions. *Physical Review*, 127, 750-761.
- [17] Ofelt, G.S. (1962) Intensities of Crystal Spectra of Rare Earth Ions. *The Journal of Chemical Physics*, 37, 511.
- [18] Sinha, S.P. (1983). Systematics and properties of lanthanides, Reidel, Dordrecht.
- [19] Krupke, W.F. (1974). *IEEE J. Quantum Electron* QE, 10, 450.
- [20] Krishnaiah, K.V., Kumar, K.U. and Jayasankar, C.K. (2013). Spectroscopic properties of  $\text{Dy}^{3+}$ -doped oxyfluoride glasses for white light emitting diodes. *Materials Express*, Vol. 3, No. 1, 61-70.
- [21] Sekhar, M.C., Rao, B.A., Barik, M.G., Reddy, A.P., Rao, P.R., Jayasankar, C.K. and Veeraiyah, N. (2012). Emission characteristics of  $\text{Dy}^{3+}$  ions in lead antimony borate glasses. *Appl. Phys. B*: 108, 455.
- [22] Naik, P.S. Ram, Ravi Babu, Y. N. Ch, Kumar, M.K. and A. Suresh Kumar, A.S. (2014). Spectral Studies of  $\text{Dy}^{3+}$  Doped Heavy Metal Oxide Glasses *I.J.C.E.T.*, 4, 5, 34734-79.
- [23] Meena, S.L. and Bhatia, B. (2016). Spectroscopic Properties of  $\text{Ho}^{3+}$  Doped Zinc Lithium Bismuth Borate Glasses, *International Journal of Engineering Science Invention*, 5, 33-37.
- [24] Meena, S. L. (2018). Spectral and Thermal Properties of  $\text{Tb}^{3+}$  Doped in Lead Lithium Borophosphate Glasses. *I.J.C.P.S.* Vol. 7, No. 6, 1-8.